Available online at www.sciencedirect.com
ScienceDirect
Trans. Nonferrous Met. Soc. China 20(2010) 2118−2123
Transactions of Nonferrous Metals Society of China
www.tnmsc.cn

Effect of Zn content on tensile and electrochemical properties of 3003 Al alloy

ZHU Mei-jun(朱美俊)[1], DING Dong-yan(丁冬雁)[1], GAO Yong-jin(高勇进)[2],
CHEN Guo-zhen(陈国桢)[2], LI Ming(李 明)[1], MAO Da-li(毛大立)[1]

1. State Key Laboratory of Metal Matrix Composites, School of Materials Science and Engineering, Shanghai Jiao Tong University, Shanghai 200240, China;
2. Huafon Al Co., Ltd, Shanghai 201506, China

Received 23 October 2009; accepted 5 August 2010

Abstract: The effect of Zn addition on the microstructure, tensile properties and electrochemical properties of as-annealed 3003 Al alloy was investigated through TEM observations, tensile tests and Tafel polarization analysis. High density precipitates are observed in the Zn-containing alloys and the alloy with 1.8% Zn addition also has rod-like precipitates. Tensile test results indicate that Zn has a great effect on tensile strength of 3003 Al alloy. The alloy with 1.5% Zn addition has the highest ultimate tensile strength. The electrochemical results indicate that Zn addition to 3003 Al alloy also has great impact on the corrosion potential of the 3003 Al alloy in 0.5% NaCl solution and ethylene glycol-water solution. The corrosion potential varies with the Zn content and shifts negatively.

Key words: 3003 Al alloy; Zn; microstructure; tensile properties; corrosion

1 Introduction

Aluminum and its alloys are important metallic materials for wide applications in various areas. Due to its low cost, high specific strength, high thermal conductivity as well as good corrosion resistance, 3003 Al alloy has been widely used for automotive heat exchangers to replace more traditional materials like stainless steels and copper alloys[1−2].

It is well known that alloying elements have a strong influence on the microstructure and properties of 3003 Al alloys. Numerous investigations were carried out to study the effect of alloying elements (such as Fe, Si and Cu) on the Mn solubility in aluminum-based solid solution and precipitation of dispersoids[3−8]. It was found that Fe and Si greatly decreased the solubility of Mn in solid solutions and accelerated the precipitation rate, and Cu enhanced the decomposition of supersaturated solid solution[9]. It was reported that Fe promoted the precipitation of Al_6(Mn, Fe) phase, while Si promoted the precipitation of α-$Al_{12}Mn_3Si$ or Al_{12}(Mn, Fe)$_3$Si (when Fe coexists)[10−11]. The size, quantity and distribution of these particles could affect the properties of 3003 Al alloy through certain mechanisms. MOORE et al[12] investigated Al alloys containing various kinds of second phases enriched with Mn, Zr, Fe or Cu and identified their different effects on the corrosion of Al alloys. FONLUPT et al[13] investigated the role of second phase in stress corrosion cracking (SCC) of an Al-Cu alloy. It was shown that the SCC susceptibility of the alloy increased with increasing quantity of the second phase particles at grain boundaries. However, the influence of Zn, especially the Zn content, on the microstructure and properties of 3003 Al alloy was rarely reported.

In the present work, three kinds of 3003 Al alloy foils with or without Zn addition were fabricated. The microstructure, tensile properties and corrosion resistance of the as-annealed foils were investigated through transmission electron microscopy, tensile test and electrochemical test, respectively.

2 Experimental

The chemical compositions of the Al alloys used in this work are shown in Table 1. Three alloys contained the same amounts of Mn, Si, Fe and Cu, but different amounts of Zn. Corresponding alloy foils were produced through the same processes, i.e., casting, hot rolling and cold rolling. After a finish rolling, all the alloy foils (with a thickness of 0.1 mm) were annealed at 380 °C for 2 h.

Corresponding author: DING Dong-yan; Tel/Fax: +86-21-34202741; Email: dyding@sjtu.edu.cn
DOI: 10.1016/S1003-6326(09)60427-1

Table 1 Chemical compositions of alloys (mass fraction, %)

Alloy	Mn	Si	Fe	Cu	Zn	Al
3003 Al	1.6	0.6	0.7	0.15	0	Bal.
3003 Al+1.5Zn	1.6	0.6	0.7	0.15	1.5	Bal.
3003 Al+1.8Zn	1.6	0.6	0.7	0.15	1.8	Bal.

Microstructures of the as-annealed alloys were observed through TEM observation. The specimens for TEM analysis were prepared through electrolytic polishing in $HClO_4$ and methanol solutions, followed by ion beam thinning. Tensile specimens were machined from the annealed alloy foils. Tensile tests at room temperature were then carried out at a tensile rate of 1 mm/min, and five specimens were taken for each alloy. Ultimate tensile strength and elongation were measured. The fracture surfaces were observed with scanning electron microscope (SEM).

Specimens for the electrochemical testing were degreased with acetone and rinsed in distilled water. Three specimens for each test were used to confirm the experimental results. All the electrochemical tests were carried out at room temperature with two electrolyte solutions. One was a 0.5% NaCl solution, and the other was 50% ethylene glycol+50% distilled water (volume fraction) with 100×10^{-6} Cl^-, which was similar to the automotive coolant. Tafel measurements were performed on a three-electrode system through a CHI660C Interface. The specimen, saturated calomel electrode (SCE) and a platinum plate were used as the working electrode, reference electrode and counter electrode, respectively. The potential sweep rate was 1 mV/s. All potentials were reported versus that of the SCE.

3 Results and discussion

3.1 Microstructure

Fig.1(a) presents the TEM images of precipitates in the as-annealed 3003 Al alloy. Dispersoids with various sizes ranging from several nanometers to about 100 nm could be found. Most of the particles have ellipsoidal shapes and precipitate inside the grain and only a few particles precipitate at the grain boundaries (Fig.1(b)). Fig.2 indicates that numerous particles distribute inside the grains of the 3003Al+1.5Zn alloy and have a spheroid shape. Fig.3 reveals that different kinds of particles precipitate in the 3003Al+1.8Zn alloy. Besides some spherical particles, quite a few rod-like particles are also observed. By comparing the precipitations in the three alloys above, it is found that the particle density and uniformity are different for different alloys, and the 3003Al+1.5Zn alloy has a much more uniform precipitates. Fig.4 presents the EDX analysis result of the

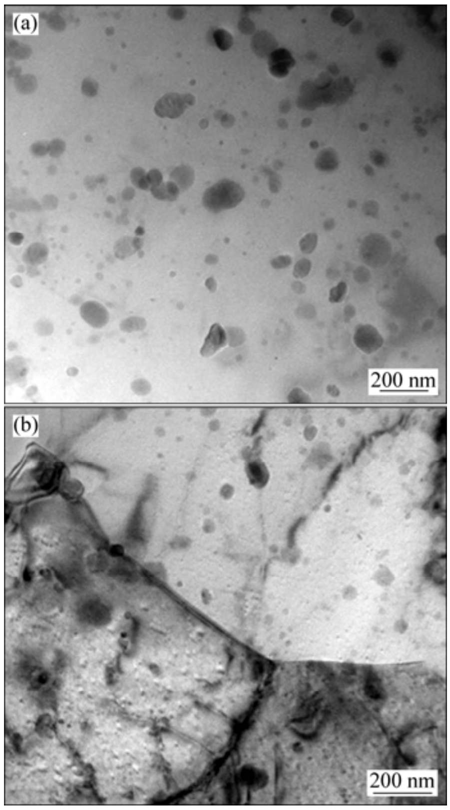

Fig.1 TEM images of 3003 Al alloy showing precipitates inside grains (a) and at grain boundaries (b)

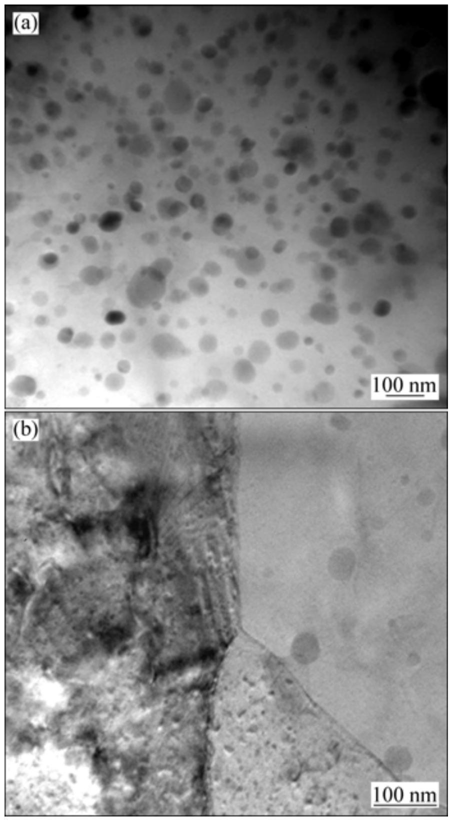

Fig.2 TEM images of 3003Al+1.5Zn alloy showing precipitates inside grains (a) and at grain boundaries (b)

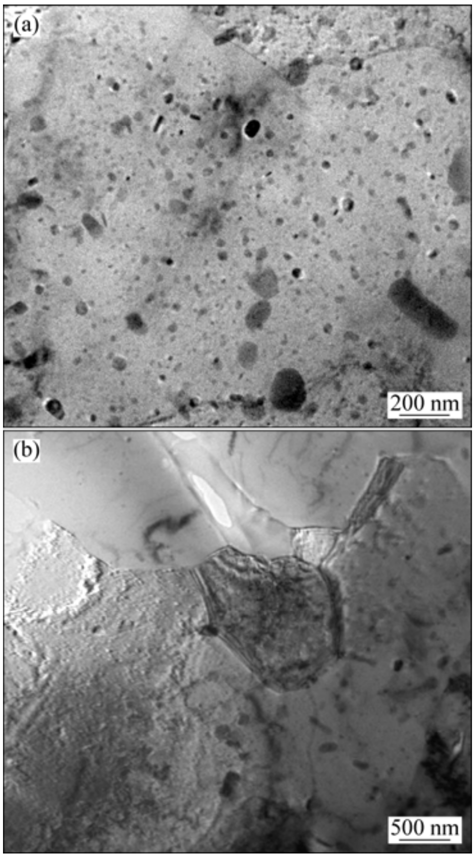

Fig.3 TEM images of 3003Al+1.8Zn alloy showing precipitates inside grains (a) and at grain boundaries (b)

dispersed particles, which mainly contain Al, Mn, Si elements and/or Cu and Zn elements.

3.2 Tensile properties

Tensile test results of the three as-annealed alloys are shown in Table 2 and Fig.5. The 3003Al+1.5Zn alloy has the highest ultimate tensile strength, but the elongation of this alloy is the lowest. The 3003Al+1.8Zn alloy has the most balanced mechanical properties to account for σ_b and δ. Obviously, the addition of 1.5% Zn to 3003 Al alloy could greatly enhance the tensile strength of the alloy, but results in a decrease of elongation of the alloy. The addition of 1.8% Zn could not only enhance the tensile strength of 3003Al alloy but also prevents a remarkable decrease of the elongation.

The difference in the tensile strength of the three alloys could be explained by different strengthening mechanisms. It is well known that there are several common strengthening mechanisms including strain strengthening, solid-solution strengthening, grain-refining strengthening and precipitation or particle strengthening. In this work, all the alloy foils were fabricated through the same rolling (strain/deformation) process, and there was no much difference in the grain size of the three alloys according to our TEM observations. Thus, strain strengthening and grain-refining strengthening should not cause the difference in tensile strength. In addition, the solid-solution hardening is limited in the 3003Al-based alloys due to the low solubility of the alloying elements. Therefore, the strength difference of the three alloys should be mainly related to the precipitation/particle strengthening mechanism. As shown above, the quantity and types of dispersoids change with the addition of Zn element, and the tensile strength changes accordingly. The enhanced tensile strength due to Zn addition should be closely related to a precipitation strengthening.

Table 2 Tensile test results of alloys

Alloy	Tensile strength/MPa	Elongation/%
3003 Al	133.05±2.57	7.47±0.75
3003Al+1.5Zn	160.22±4.43	4.18±0.79
3003Al+1.8Zn	154.48±5.03	7.04±0.71

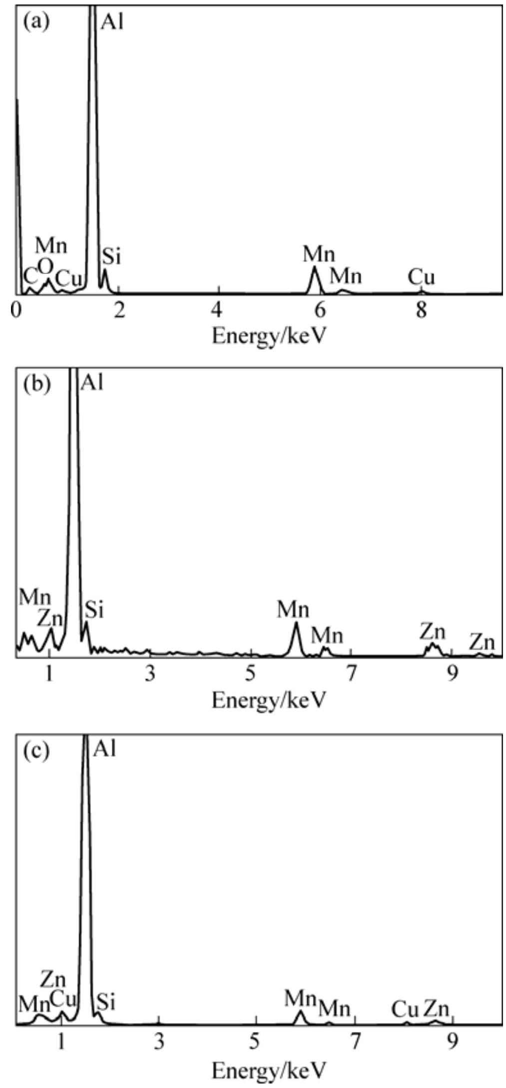

Fig.4 EDX spectra of dispersed particles in 3003Al alloy (a), 3003Al+1.5Zn alloy (b) and 3003Al+1.8Zn alloy (c)

The tensile fracture surfaces of the three as-annealed alloys are shown in Figs.6−8. A large quantity of dimples is observed in all the alloys, which indicates that the tensile fracture mode is a typical ductile fracture. The dimples vary in size. The larger dimples may form (around bigger inclusions) during the early stage of deformation and expand with the increase of displacement, while the finer ones may nucleate around relatively small particles in the later stage of tensile deformation.

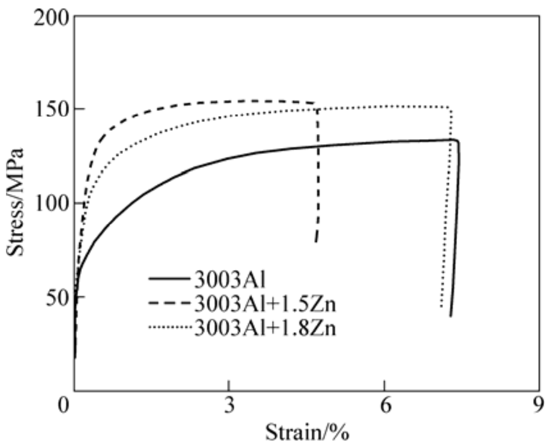

Fig.5 Stress—strain curves of as-annealed alloys

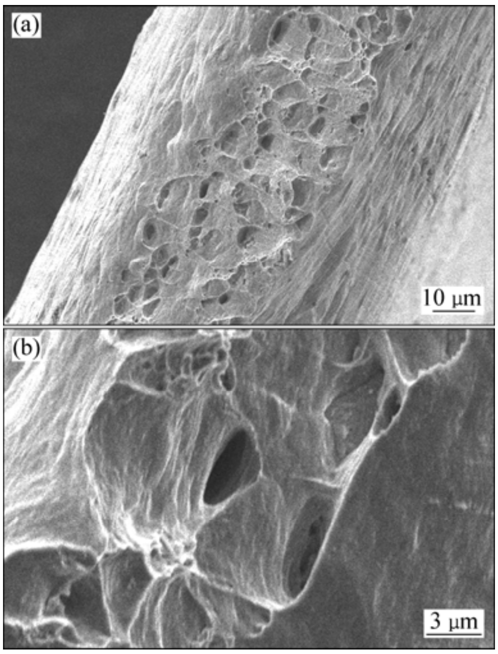

Fig.6 Fractured surface morphologies of 3003 Al alloy: (a) Low magnification; (b) High magnification

3.3 Electrochemical properties

Fig.9 shows the room-temperature polarization curves of 3003 Al, 3003Al+1.5Zn and 3003Al+1.8Zn alloys in the NaCl solution and the ethylene glycol-water solution, respectively. The corrosion potential and corrosion current density are listed in Table 2. It could be

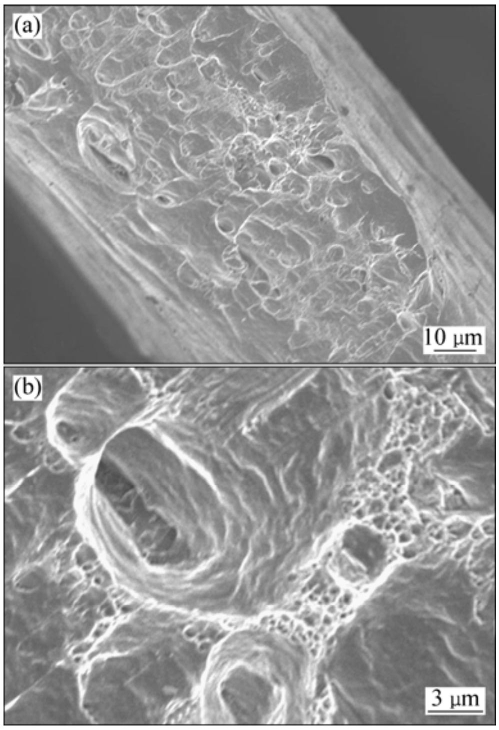

Fig.7 Fracture surface morphologies of 3003Al+1.5Zn alloy: (a) Low magnification; (b) High magnification

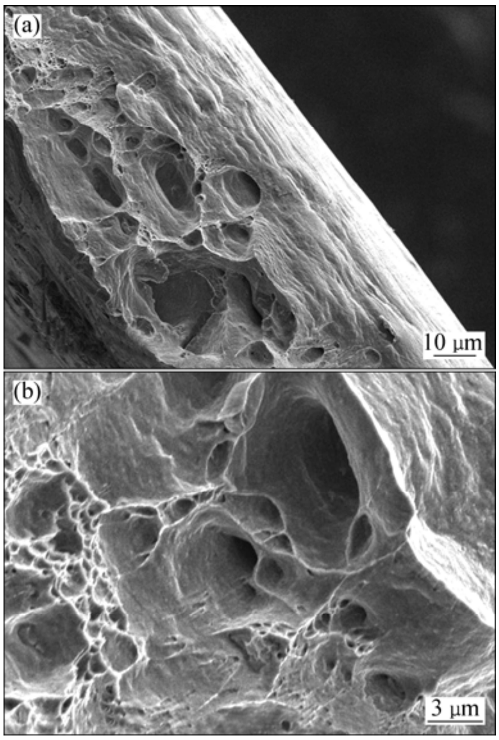

Fig.8 Fractured surface morphologies of 3003Al+1.8Zn alloy: (a) Low magnification; (b) High magnification

found that the corrosion potential of both 3003Al+1.5Zn alloy and 3003Al+1.8Zn alloys is more negative than that of 3003Al alloy, and the corrosion potential of 3003Al+1.8Zn aluminum alloy is higher than that of

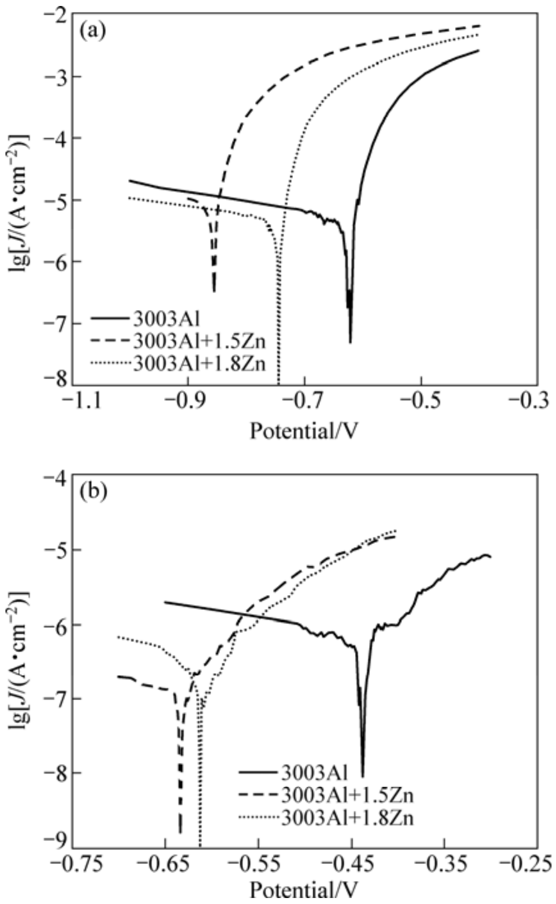

Fig.9 Tafel polarization plots of alloys: (a) In 0.5%NaCl solution; (b) In ethylene glycol-water solution

Table 2 Tafel polarization parameters of alloys in different solutions

Electrolyte solution	Alloy	φ_{corr}(vs SCE)/mV	J_{corr}/($\mu A \cdot cm^{-2}$)
0.5%NaCl	3003 Al	−622	6.560
	3003Al+1.5Zn	−855	13.77
	3003Al+1.8Zn	−744	13.60
Ethylene glycol-water	3003 Al	−438	0.225
	3003Al+1.5Zn	−633	0.966
	3003Al+1.8Zn	−612	0.991

3003Al+1.5Zn alloy. The polarization curves of 3003 Al, 3003Al+1.5Zn and 3003Al+1.8Zn alloys in the ethylene glycol-water solution are similar to those tested in the NaCl solution. However, all the alloys in the ethylene glycol-water solution have a higher corrosion resistance than those in the NaCl solution. This suggests that the addition of Zn to 3003 Al alloy would decrease the corrosion resistance of 3003 Al alloy in the above two solutions. Figs.10−12 present the surface morphologies of the corroded alloys in two solutions. It could be found that 3003Al+1.5Zn alloy is more severely corroded in the 0.5%NaCl solution during the electrochemical test. No obvious corrosion is observed in the ethylene glycol-water solution, which suggests that the corrosion

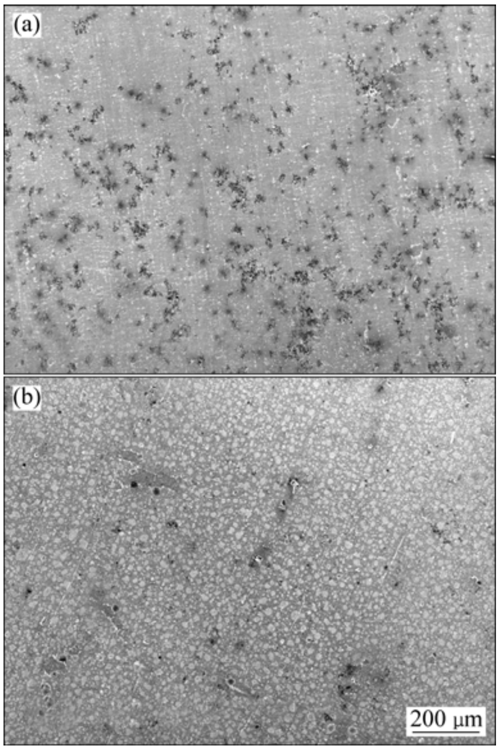

Fig.10 Corrosion surface morphologies of 3003 Al alloy after polarization test in (a) 0.5%NaCl solution and (b) ethylene glycol-water solution

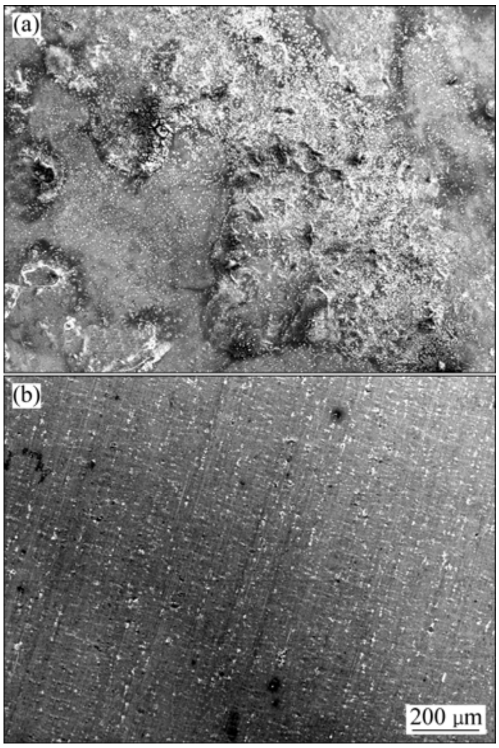

Fig.11 Corrosion surface morphologies of 3003Al+1.5Zn alloy after polarization test in 0.5%NaCl solution (a) and ethylene glycol-water solution (b)

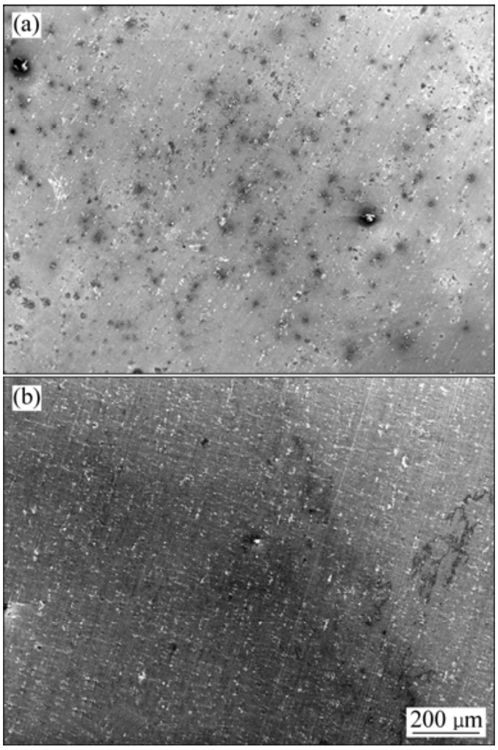

Fig.12 Corrosion surface morphologies of 3003Al+1.8Zn alloy after polarization testing in 0.5%NaCl solution (a) and ethylene glycol-water solution (b)

in the latter solution is lighter than that in the NaCl solution. A large quantity of particles could be seen on the corroded surface, as seen in Fig.11(a), which implies that the corrosion resistance is highly related to the quantity of particles. The more dispersoids the alloy contains, the stronger the corrosion sensitivity of the alloy is[14]. It could be predicted that the shapes of the particles also have an influence on the corrosion property of the alloy. The dispersoids with rod-like shape could cause more severe lattice distortion than spherical particles and thus form microcracks during the rolling process[15−16]. Therefore, easy corrosion could initiate in the surroundings of rod-like dispersoids.

4 Conclusions

1) For the three as-annealed alloys, high density particles precipitate inside the grains and only a few precipitate at the grain boundaries. The 3003Al+1.5Zn alloy has a uniform precipitation behavior and some rod-like precipitates are also observed in the 3003Al+1.8Zn alloy.

2) Zn has a strong influence on the tensile strength of the 3003 Al alloy. The 3003Al+1.5Zn alloy has the highest ultimate tensile strength but the lowest elongation. The 3003Al+1.8Zn alloy presents the most balanced mechanical properties.

3) Zn has a great impact on the corrosion resistance of 3003 Al alloy. It causes a negative shift of the corrosion potential of the 3003 Al alloy.

References

[1] MILLER W S, ZHUANG L, BOTTEMA J, WITTEBROOD A J, de SMET P, HASZLER A, VIEREGGE A. Recent development in aluminium alloys for the automotive industry [J]. Material Science and Engineering A, 2000, 280(1): 37−49.

[2] GEOFF D. Materials for automobile bodies [M]. Oxford: Butterworth-Heinemann, 2003: 1−90.

[3] GOEL D B, FURRER P, WARLIMONT H. Precipitation in aluminum manganese (iron, copper) alloys [J]. Aluminium, 1974, 50(8): 511−516.

[4] SHI Yao-wu, YU Yang, XIA Zhi-dong, LEI Yong-ping, LI Xiao-yan, GUO Fu, LIU Jian-ping. Study on Al-Cu-Si braze containing small amount of rare earth erbium [J]. Frontiers of Materials Science in China, 2008, 2(4): 351−356. (in Chinese)

[5] FERNANDES R C, PADILHA A F. Effect of Mn and Fe contents on the microstructural evolution of two twin roll caster Al-Fe-Mn-Si alloys [J]. Rem-revista Escola De Minas, 2008, 61(2): 165−169.

[6] MARTINS J P, CARVALHO A L M, PADILAHA A F. Microstructure and texture assessment of Al-Mn-Fe-Si (3003) aluminum alloy produced by continuous and semicontinuous casting processes [J]. Journal of Materials Science, 2009, 44(11): 2966−2976.

[7] KIM I, AKRAMOV S, JEONG H B. Texture and formability development of asymmetry rolled AA 3003 Al alloy sheet [J]. International Journal of Modern Physics B, 2008, 21(31): 5895−5900.

[8] HUANG H W, OU B L. Evolution of precipitation during different homogenization treatments in a 3003 aluminum alloy [J]. Materials and Design, 2009, 30(7): 2685−2692.

[9] LI Y J, ARNBERG L. Quantitative study on the precipitation behavior of dispersoids in DC-cast AA3003 alloy during heating and homogenization [J]. Acta Materialia, 2003, 51(12): 3415−3428.

[10] NES E, NAESS S E, HOIER R. Decomposition of an aluminium-manganese alloy [J]. Z Metallk, 1972, 63(5): 248−252.

[11] LODGAARA L, RYUM N. Precipitation of dispersoids containing Mn and/or Cr in Al-Mg-Si alloys [J]. Material Science and Engineering A, 2000, 283(1/2): 144−152.

[12] MOORE K L, SYKES J M, HOGG S C, GRANT P S. Pitting corrosion of spray formed Al-Li-Mg alloys [J]. Corrosion Science, 2008, 50(11): 3221−3226.

[13] FONLUPT S, BAYLE B, DELAFOSSE D, HEUZE J. Role of second phases in the stress corrosion cracking of a nickel-aluminium bronze in saline water [J]. Corrosion Science, 2005, 47(11): 2792−2806.

[14] LUNDER O, NISANCIOGLU K. The effect of alkaline-etch Pretreatment on the pitting corrosion of wrought aluminum [J]. Corrosion Science, 1988, 44(7): 414−422.

[15] JIN Li, ZHANG Xin-ming, TANG Jian-guo, YOU Jiang-hai, ZHOU Zhou-ping. Effect of high temperature annealing on corrosion property of cathode aluminium foils [J]. The Chinese Journal of Nonferrous Metals, 2003, 13(2): 424−427. (in Chinese)

[16] LIU Y, CHENG Y F. Role of second phase particles in pitting corrosion of 3003 Al alloy in NaCl solution [J]. Materials and Corrosion, 2010, 61(3): 211−217. (in Chinese)

(Edited by FANG Jing-hua)